



HAL
open science

Deep Learning-Based Neuromelanin MRI Changes of Isolated REM Sleep Behavior Disorder

Rahul Gaurav, Nadya Pyatigorskaya, Emma Biondetti, Romain Valabrègue, Lydia Yahia-cherif, Graziella Mangone, Smaranda Leu-semenescu, Jean-christophe Corvol, Marie Vidailhet, Isabelle Arnulf, et al.

► **To cite this version:**

Rahul Gaurav, Nadya Pyatigorskaya, Emma Biondetti, Romain Valabrègue, Lydia Yahia-cherif, et al.. Deep Learning-Based Neuromelanin MRI Changes of Isolated REM Sleep Behavior Disorder. Movement Disorders, 2022, 10.1002/mds.28933 . hal-03552782

HAL Id: hal-03552782



<https://hal.sorbonne-universite.fr/hal-03552782v1>

Submitted on 2 Feb 2022

HAL is a multi-disciplinary open access archive for the deposit and dissemination of scientific research documents, whether they are published or not. The documents may come from teaching and research institutions in France or abroad, or from public or private research centers.

L'archive ouverte pluridisciplinaire **HAL**, est destinée au dépôt et à la diffusion de documents scientifiques de niveau recherche, publiés ou non, émanant des établissements d'enseignement et de recherche français ou étrangers, des laboratoires publics ou privés.

Deep Learning-Based Neuromelanin MRI Changes of Isolated REM Sleep Behavior Disorder

Rahul Gaurav, MS, PhD,^{1,2,3*} 
 Nadya Pyatigorskaya, MD, PhD,^{1,2,3,4}
 Emma Biondetti, PhD,^{1,2,3} Romain Valabrègue, PhD,^{1,2}
 Lydia Yahia-Cherif, PhD,^{1,2} Graziella Mangone, MD, PhD,^{2,5}
 Smaranda Leu-Semenescu, MD,⁷
 Jean-Christophe Corvol, MD, PhD,^{2,4,6} 
 Marie Vidailhet, MD,^{2,3,6} Isabelle Arnulf, MD, PhD,^{1,3,7} 
 and Stéphane Lehéricy, MD, PhD^{1,2,3,5}

¹Center for NeuroImaging Research (CENIR), Paris Brain Institute—ICM, Paris, France ²Sorbonne Université, Paris Brain Institute—ICM, INSERM U1127, CNRS UMR 7225, Pitié-Salpêtrière Hospital, Paris, France ³Movement Investigations and Therapeutics—MOV'IT Team, Paris Brain Institute—ICM, Paris, France ⁴Department of Neuroradiology, Pitié-Salpêtrière Hospital, AP-HP, Paris, France ⁵INSERM, Clinical Investigation Center for Neurosciences (CIC), Pitié-Salpêtrière Hospital, Paris, France ⁶Department of Neurology, Pitié-Salpêtrière Hospital, AP-HP, Paris, France ⁷Sleep Disorders Unit, Pitié-Salpêtrière Hospital, AP-HP, Paris, France

This is an open access article under the terms of the Creative Commons Attribution-NonCommercial-NoDerivs License, which permits use and distribution in any medium, provided the original work is properly cited, the use is non-commercial and no modifications or adaptations are made.

*Correspondence to: Dr. Rahul Gaurav, Centre de NeuroImagerie de Recherche – CENIR, Institut du Cerveau – ICM, Hôpital Pitié-Salpêtrière, 47 Boulevard de l'Hôpital, 75013 Paris, France; E-mail: rahul.gaurav@icm-institute.org

Relevant conflicts of interest/financial disclosures: R.G. and S.L. received grant funding from Biogen. E.B. received grant funding from France Parkinson and Biogen. R.V., N.P., G.M., L.Y.C., S.L.S., and M.V. have nothing to report. J.C.C. has served in advisory boards for Air Liquide, Biogen., Denali, Ever Pharma, Idorsia, Prevail Therapeutic, TheraNexus, and UCB; has received grants from Sanofi and The Michael J. Fox Foundation. I.A. received honoraria from Idorsia Pharma unrelated to this study.

Funding agencies: This study was funded by grants from the Investissements d'Avenir, IAIHU-06 (Paris Institute of Neurosciences, IHU), ANR-11-INBS-0006, ERA PerMed EU-wide project DIGIPD (01KU2110), Fondation d'Entreprise EDF, Biogen, Fondation Thérèse and René Planiol, Fondation Saint Michel, unrestricted support for research on Parkinson's disease from Energipole (M. Mallart), M. Villain, and Société Française de Médecine Esthétique (M. Legrand). This work was supported by grants from DHOS-Inserm, France Parkinson, Ecole des NeuroSciences de Paris (ENP), and Fondation pour la Recherche Médicale (FRM).

Received: 20 May 2021; **Revised:** 6 January 2022; **Accepted:** 9 January 2022

Published online in Wiley Online Library (wileyonlinelibrary.com). DOI: 10.1002/mds.28933

ABSTRACT: Background: Isolated REM sleep behavior disorder (iRBD) is considered a prodromal stage of parkinsonism. Neurodegenerative changes in the substantia nigra pars compacta (SNc) in parkinsonism can be detected using neuromelanin-sensitive MRI.

Objective: To investigate SNc neuromelanin changes in iRBD patients using fully automatic segmentation.

Methods: We included 47 iRBD patients, 134 early Parkinson's disease (PD) patients and 55 healthy volunteers (HVs) scanned at 3 Tesla. SNc regions-of-interest were delineated automatically using convolutional neural network. SNc volumes, volumes corrected by total intracranial volume, signal-to-noise ratio (SNR) and contrast-to-noise ratio were computed. One-way general linear models (GLM) analysis of covariance (ANCOVA) was conducted while adjusting for age and sex.

Results: All SNc measurements differed significantly between the three groups (except SNR in iRBD). Changes in iRBD were intermediate between those in PD and HVs.

Conclusions: Using fully automated SNc segmentation method and neuromelanin-sensitive imaging, iRBD patients showed neurodegenerative changes in the SNc at a lower level than in PD patients. © 2022 The Authors. *Movement Disorders* published by Wiley Periodicals LLC on behalf of International Parkinson and Movement Disorder Society

Key Words: substantia nigra; neuromelanin; isolated REM sleep behavior disorder; parkinsonism; convolutional neural networks; deep learning; artificial intelligence

Introduction

Isolated rapid eye movement (REM) sleep behavior disorder (iRBD) is characterized by abnormal behaviors and loss of normal muscle atonia during REM sleep, without daytime neurological disorders. Previous studies have suggested that most iRBD subjects will develop Parkinson's disease (PD) or dementia with Lewy bodies (DLB) with a median conversion time of 7 years.^{1,2} At PD onset, 30% to 60% of the dopaminergic neurons in the substantia nigra pars compacta (SNc) are already lost.^{3,4} Because most of the iRBD subjects are in a prodromal parkinsonism stage, they present mild SNc impairment as shown using transcranial sonography,⁵ and magnetic resonance imaging (MRI) with a loss of the dorsolateral nigral hyperintensity,^{6,7} diffusion changes,^{2,8} and disruption of basal ganglia connectivity.⁹ Reduced striatal dopaminergic function was also reported.^{5,10}

Neurodegenerative changes in the SNc can be studied using neuromelanin-sensitive MRI. Neuromelanin is a pigment contained in SNc dopaminergic neurons that acquires paramagnetic properties when associated with metals, therefore, becoming visible using MRI.¹¹ Concordant studies have reported reduced SNc size and signal intensity in PD using neuromelanin-sensitive imaging with high diagnostic accuracy.¹²⁻¹⁴ Changes predominated in the ventral posterolateral SN.¹⁵ Only two studies have used neuromelanin-sensitive MRI to study the SNc changes in iRBD in a small number of patients without any comparison with PD patients,² or in a larger number, but at a group level.¹⁶ Both studies used manual SNc segmentation, a method that is dependent on the experimenter training.

Here, we investigated neuromelanin signal changes in a large group of patients with iRBD as compared to PD patients and healthy volunteers (HVs) by automatically segmenting the SNc using a convolutional neural network (ConvNet)-based architecture called the U-net.¹⁷ For methodological validation, the automated measurements were compared with the manual ones.

Subjects and Methods

Subjects were prospectively recruited from May 2015 to March 2020 as part of the ICEBERG study (ClinicalTrials.gov: NCT02305147). For inclusion, patients were clinically diagnosed by a movement disorder specialist, with an age range between 18 and 75 years, had no/minimal cognitive disturbances, and a disease duration <4 years. Patients with iRBD met the international diagnostic criteria for RBD and had no parkinsonism or cognitive disturbances, nor did they take any drug that could increase muscle tone during REM sleep.^{18,19} We confirmed RBD using video polysomnography in all cases, following the International Classification of Sleep Disorders-3 criteria, by sleep neurologists (I.A. and S.L.S.). The isolated character of RBD was ascertained in absence of the MDS criteria for PD, multiple system atrophy and DLB, by three movement disorders specialists (M.V., G.M., and J.C.C.). HVs had no history of neurological or psychiatric disorders. The local ethics committee approved this study and all subjects provided written informed consent (IRB of Paris VI, RCB 2014-A00725-42).

Subjects were scanned at 3 Tesla (PRISMA, Siemens, Germany) using a 64-channel head coil. The MRI protocol included whole brain three-dimensional (3D) T1-weighted (T1-w) imaging (sagittal MP2RAGE with a 1-mm isotropic resolution) and two-dimensional (2D) T1-w neuromelanin-sensitive imaging (axial turbo spin echo [TSE] with pulse repetition time [TR]/echo time [TE]/flip angle: 890 ms/13 ms/180°, 3 averages, voxel size: 0.4 × 0.4 × 3 mm³).

Image analysis was performed in MATLAB (vR2017b; The MathWorks, Natick, MA, USA) using FSL (FMRIB v5.0; Oxford, UK) and Statistical Parametric Mapping (SPM12; London, UK). Image preprocessing and post-processing were performed using MRtrix (v3.0.1).

For manual segmentation, SNc and background contours were delineated using FreeSurfer viewer (v5.3.0; MGH, USA) on the neuromelanin-sensitive images by two independent trained raters blind to the subject's clinical status as described previously (Supplementary Fig. S1).²

For automatic segmentation, a deep learning pipeline was implemented in Python 3.6.0 (Data S1). From the 236 manually segmented images, a random dataset of 60 images was randomly split into 54 principal training images and six external validation images. We ran the U-net model to predict the SNc ROI fully automatically on the remaining 176 external subjects that were excluded during the training phase.

We calculated SNc volumes (Vol), corrected volume ($C_{vol} = Vol/total\ intracranial\ volume$) to normalize for the subject head size, signal-to-noise ratio (SNR) and contrast-to-noise ratio (CNR) by normalizing the mean signal in SNc relative to the background signal, as described in previous studies (Data S1).^{2,20} Statistical analyses were performed using R (R Core Team 2019, v3.6.1) and MATLAB. The between-group comparisons of demographic and clinical variables were performed using the parametric Student's *t* test. Sex proportions were assessed using the χ^2 test. Between-group differences in Vol, C_{vol} , SNR, and CNR were evaluated using one-way general linear model (GLM) analysis of covariance (ANCOVA) by keeping group (iRBD, PD, and HV) as the only between-group factor while treating both sex and age as covariates and also by using post hoc *t* tests. Receiver operating characteristic (ROC) analysis was performed to obtain a diagnostic value. Dice similarity co-efficient and intraclass correlation coefficient (ICC) was computed to evaluate the overall segmentation performance by comparing the automatic and manual segmentations.

We calculated the Pearson's correlation coefficients between the SNc measurements and both age and clinical scores. An approximate multivariate permutation test was performed to adjust for multiple comparisons.²¹

Results

We analyzed 236 participants comprising 47 subjects with iRBD, 134 with PD, and 55 HVs. Patients with iRBD were older than HVs ($P < 0.001$) and there was no significant difference in age between PD and HVs. There was a larger proportion of males among iRBD and PD patients than in HVs ($\chi^2 = 16.484$, $P < 0.001$). Using both methods, we observed a significant sex effect in C_{vol} between the three groups and in CNR

TABLE 1 Demographic, clinical characteristics and SNc measurements

Demographics	HV _s	iRBD	PD	t test ^a (P value)							
				HV _s vs. iRBD	iRBD vs. PD						
No. of subjects	55	47	134								
Age, y	61.4 ± 8.8	67.7 ± 5.0 ^{b,c}	61.6 ± 9.4	0.90	<0.001						
Male/Female	27/28	41/6 ^{b,c}	84/50	0.84	<0.001						
Clinical characteristics											
MMSE	29.4 ± 0.8	29.0 ± 1.0 ^d	29.0 ± 1.2 ^c	0.01	0.01						
MDS-UPDRS I	5.1 ± 3.4	8.9 ± 4.9 ^b	9.4 ± 3.9 ^f	<0.001	<0.001						
MDS-UPDRS II	1.2 ± 1.8	2.3 ± 2.2 ^{b,c}	8.1 ± 3.8 ^c	<0.001	0.00						
MDS-UPDRS III off	5.7 ± 5.4	11.7 ± 6.5 ^{b,c}	29.5 ± 7.9 ^f	<0.001	<0.001						
MDS-UPDRS IV	NA	NA	0.1 ± 0.7	NA	NA						
Hoehn and Yahr score	0.1 ± 0.5	0.7 ± 0.9 ^{b,c}	2.0 ± 0.3 ^f	<0.001	<0.001						
GLM-ANCOVA: group factor											
SNc imaging measurements Automated		HV _s vs. iRBD	PD vs. iRBD	HV _s vs. PD		iRBD vs. PD					
				F value	P value	F value	P value	F value	P value		
Volume (mm ³)	297.1 ± 55.1	240.3 ± 47.5 ^{b,g}	218.8 ± 51.0 ^f	44.32	<0.001	85.39	<0.001	29.85	<0.001	6.18	0.01
Corrected volume (C _{vol})	0.21 ± 0.04	0.16 ± 0.04 ^{b,g}	0.15 ± 0.04 ^f	51.00	<0.001	99.29	<0.001	31.47	<0.001	8.16	0.00
SNR	110.1 ± 1.5	109.7 ± 1.9 ^c	108.4 ± 1.5 ^f	25.70	<0.001	47.27	<0.001	1.79	0.18	20.40	<0.001
CNR	1.58 ± 0.27	1.45 ± 0.34 ^{d,g}	1.30 ± 0.30 ^f	18.34	<0.001	37.74	<0.001	4.80	0.03	8.28	0.00
Manual											
Volume (mm ³)	261.8 ± 41.3	229.5 ± 26.3 ^b	217.9 ± 56.3 ^f	16.06	<0.001	27.50	<0.001	21.41	<0.001	1.82	0.17
Corrected volume (C _{vol})	0.18 ± 0.03	0.16 ± 0.02 ^b	0.14 ± 0.04 ^f	21.74	<0.001	38.31	<0.001	20.61	<0.001	3.37	0.07
SNR	111.1 ± 1.5	110.7 ± 1.7 ^c	109.4 ± 1.6 ^f	25.75	<0.001	43.39	<0.001	1.68	0.20	21.38	<0.001
CNR	1.74 ± 0.28	1.60 ± 0.33 ^{d,g}	1.46 ± 0.34 ^f	16.05	<0.001	30.94	<0.001	5.20	0.02	6.76	0.01

Demographical and clinical characteristics were compared using t-tests. Significant differences are indicated in italics. Data represented as mean ± standard deviation.

^aSex was compared using χ^2 .

^bFor P value <0.001.

^cFor P value <0.001.

^dIndicates significant difference between HV_s and iRBD with P value <0.01.

^eIndicates significant difference between HV_s and PD with P value <0.01.

^fFor P value <0.001.

^gIndicates significant difference between iRBD and PD with P value <0.0.

Abbreviations: SNc, substantia nigra pars compacta; HV_s, healthy volunteers; iRBD, isolated REM sleep behavior disorder; PD, Parkinson's disease; MMSE, Mini-Mental State Examination; SNR, signal-to-noise ratio; CNR, contrast-to-noise ratio.

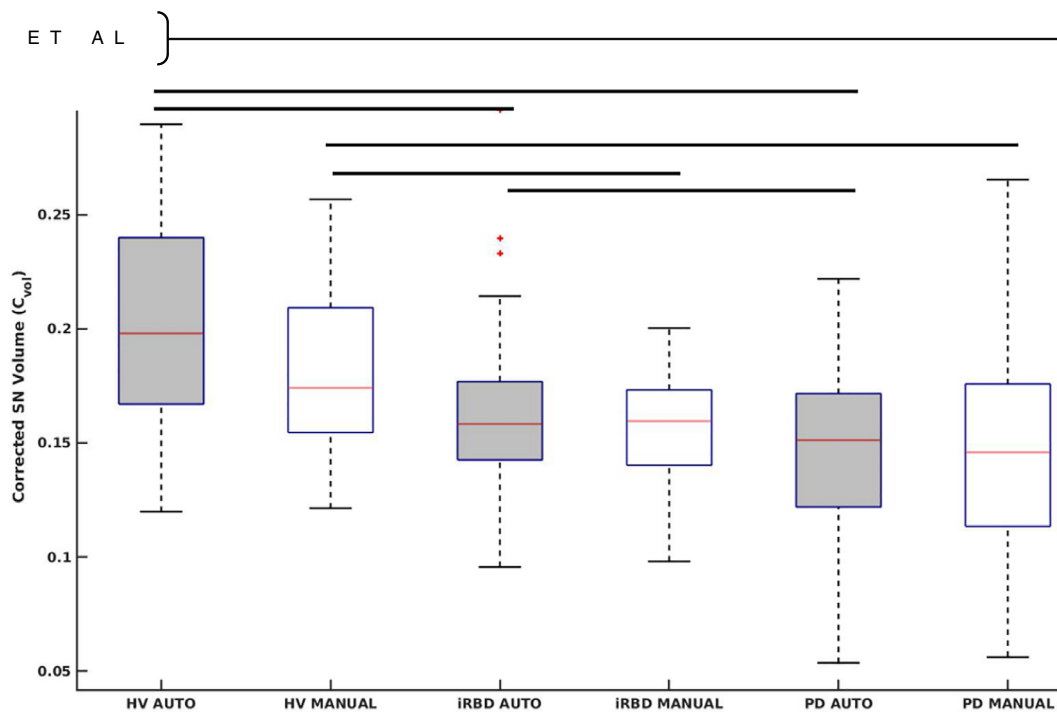


FIG. 1. Box plot of corrected substantia nigra pars compacta (SNc) volume (C_{vol}) between isolated REM sleep behavior disorder (iRBD), Parkinson's disease (PD), and healthy volunteers (HVs) using both automatic and manual segmentation methods. [Color figure can be viewed at wileyonlinelibrary.com]

between iRBD and PD groups. All three groups had significantly larger C_{vol} in females than males (F value = 23.40, P value < 0.001). All SNc measurements (Vol, C_{vol} , SNR, and CNR) differed significantly between the three groups (Table 1). Furthermore, all SNc measurements were significantly lower in PD than in both iRBD and HVs and in iRBD than in HVs except for SNR that did not differ between iRBD and HVs (Fig. 1, Table 1).

The ROC analyses provided areas under the curve of 0.78 for Vol, 0.79 for C_{vol} , 0.56 for SNR, and 0.63 for CNR between iRBD and HVs and 0.83 for Vol, 0.85 for C_{vol} , 0.79 for SNR, and 0.77 for CNR between PD and HVs (Supplementary Table S1).

The same between-group differences were obtained using the manual method. The ROC analysis results were also similar (Supplementary Table S1).

Correlation study for automated method showed the following results. Age did not correlate with any SNc measurements in any of the three groups. In the iRBD group, there were significant positive correlations between Vol and C_{vol} and Movement Disorder Society-Unified Parkinson's Disease Rating Scale (MDS-UPDRS) I and II scores and a trend for a positive correlation between C_{vol} and MDS-UPDRS III off. In PD, there were significantly negative correlations between C_{vol} and MDS-UPDRS III off score and a trend for Vol (Supplementary Table S2). Correlations for manual measurements are presented in Supplementary Table S2.

There was a high overall reproducibility between all automatic and manual segmentations ($n = 236$, Dice, 0.80; ICC for SNR, 0.75; ICC for CNR, 0.82). Similarly, high between automatic and manual

segmentations used in training (Dice, 0.80), and also between the measurements performed by the two manual raters (Dice inter-observer, 0.82, Dice intra-observer, 0.85).

Discussion

Using a robust fully automated ConvNet-based SNc segmentation method; this study confirmed that iRBD presented reduced neuromelanin content and SNc volume in a large number of subjects. The automated method demonstrated significant differences between both iRBD and PD and between iRBD and HVs separately for all SNc measurements. Volumes and signal changes were at an intermediate level between values in HVs and PD patients. All female groups had larger C_{vol} similar to previous HVs²² and PD²⁰ studies.

Neuromelanin-based SNc volume in iRBD decreased by 19.1% and SNR by 4.0% as compared to HVs. Changes were milder than in previous study possibly because of the differences in scanners, examiners, and subject characteristics (examinations performed by different neurologists using different clinical scales: UPDRS vs. MDS-UPDRS).² Changes were also milder than in the PD group, in which Vol decreased by 26.3% and SNR by 16.7%, in line with previous studies in de novo PD patients.²³⁻²⁶

SN changes observed using the automatic method were comparable to the established ground truth that was the manual method. Our model needed a small training dataset. Furthermore, the untrained testing dataset of 176 subjects was more than three times the size of the training dataset. This demonstrated the

robustness of our model that it has the potential to segment untrained external neuromelanin data from other scanners as well. Recently, various artificial intelligence (AI) models based on deep learning segmentation techniques have made tremendous progress in the field of quantitative neuroimaging analysis.^{17,27-29} Despite this breakthrough, the potential has been limited because the medical datasets were relatively small and training any AI model is a difficult task with a relatively small size of datasets.²⁷⁻²⁹ Here, the Dice coefficient between the automatic and manual method was high, similar to previous studies.²⁸ We also obtained similar SNc volume decrease between HVs and PD of 26.4% in line with a previous study using U-net model.²⁹

There was no correlation between SNc neuromelanin measures in the HVs or iRBD group and age using either of the segmentation methods, in line with previous studies demonstrating a plateau of neuromelanin in midlife from the 5th to 6th decades.^{22,30} In the iRBD group, MDS-UPDRS I and II scores correlated positively with Vol and C_{vol} and a trend was seen between C_{vol} and MDS-UPDRS III off scores. These correlations were unexpected given the negative correlations found in PD and hence, should be interpreted with caution because of the limited number of patients. These different correlations may be explained by a hypothesis derived from animal model of PD.³⁰ According to this hypothesis, neuromelanin would first accumulate in SN neurons (explaining the positive correlation). Beyond a certain threshold, this accumulation would compromise neuronal function and trigger PD-type pathology (explaining the negative correlation).

In PD, SNc volume demonstrated a trend for Vol and significantly negative correlation with MDS-UPDRS III scores in line with previous studies.³¹⁻³⁶ Many of the correlations were found using both methods (eg, MDS-UPDRS I with C_{vol} in iRBD, trend for MDS-UPDRS on with Vol in PD), but not all (eg, SN measurements and age in PD in the manual method as in our previous study,²⁰ but not in the automated method). Therefore, although overall results were broadly similar between the two methods, there were some differences that could be because of the image resampling procedure or the greater SNc segmentation provided by the automatic method.

The study had several limitations and can be improved in several ways. First, it needs to be further validated using external cohorts scanned with different scanners, which could help us understand the scanner effect using this model. Although such automatic methods have the potential advantages of saving time and being more reproducible, yet manual segmentation allows careful image quality control and removal of areas containing artifacts (eg, caused by blood flow or head motion). As a result, experienced raters can deliver highly reproducible segmentations.^{37,38} Second, the implementation of 3D acquisitions may possibly increase the accuracy of the results³⁹ by enabling isotropic voxel acquisitions,

reducing partial voluming and eliminating or reducing artifacts (eg, caused by cross-talk between slices in 2D sequences). Moreover, more clinical assessments are warranted to understand the clinical significance of SNc neuromelanin loss in iRBD.

Patients with iRBD showed a decrease in SNc volume and signal intensity, and our results confirmed that neuromelanin MRI signal is an early marker of SNc neurodegeneration in parkinsonism. Nonetheless, comparative MRI, histological and molecular studies are needed to better understand the basis of neuromelanin-based MRI signal changes in iRBD.

In summary, our proposed fully automated ConvNet segmentation method showed comparable performance with the manual method, was faster and user-independent. Therefore, it could enable reproducible and fast segmentation of the SNc in large patient cohorts, for instance, in clinical trials. Several questions still remain unanswered, in particular whether neuromelanin imaging could serve as a predictor of conversion in these patients or to estimate the time before the appearance of clinical motor signs and the evolution of neuromelanin changes in relation to the striatal dopaminergic function. ■

Acknowledgments: The authors would like to thank Energipole (M. Mallart), M. Villain and Société Française de Médecine Esthétique (M. Legrand) for unrestricted support for Research on Parkinson's disease. We would also like to thank all of the participants involved in the study, who have helped to make this research possible.

Data Availability Statement

The data that support the findings of this study are available from the corresponding author upon reasonable request.

References

1. Iranzo A, Fernández-Arcos A, Tolosa E, et al. Neurodegenerative disorder risk in idiopathic REM sleep behavior disorder: study in 174 patients. *PLoS One* 2014;9(2):e89741.
2. Pyatigorskaya N, Gaurav R, Arnaldi D, et al. Magnetic resonance imaging biomarkers to assess substantia nigra damage in idiopathic rapid eye movement sleep behavior disorder. *Sleep* 2017;40(11):1-8.
3. Poewe W, Seppi K, Tanner CM, et al. Parkinson disease. *Nat Rev Dis Prim* 2017;3:1-21.
4. Kish SJ, Shannak K, Hornykiewicz O. Uneven pattern of dopamine loss in the striatum of patients with idiopathic Parkinson's disease. *N Engl J Med* 1988;318(14):876-880.
5. Iranzo A, Lomeña F, Stockner H, et al. Decreased striatal dopamine transporter uptake and substantia nigra hyperchogenicity as risk markers of synucleinopathy in patients with idiopathic rapid-eye-movement sleep behaviour disorder: a prospective study [internet]. *Lancet Neurol* 2010;9(11):1070-1077. [https://doi.org/10.1016/S1474-4422\(10\)70216-7](https://doi.org/10.1016/S1474-4422(10)70216-7)
6. Barber TR, Griffanti L, Bradley KM, et al. Nigrosome 1 imaging in REM sleep behavior disorder and its association with dopaminergic decline. *Ann Clin Transl Neurol* 2020;7(1):26-35.
7. De Marzi R, Seppi K, Högl B, et al. Loss of dorsolateral nigral hyperintensity on 3.0 tesla susceptibility-weighted imaging in idiopathic rapid eye movement sleep behavior disorder [internet]. *Ann. Neurol* 2016;79(6):1026-1030.

8. Scherfler C, Frauscher B, Schocke M, et al. White and gray matter abnormalities in idiopathic rapid eye movement sleep behavior disorder: a diffusion-tensor imaging and voxel-based morphometry study. *Ann Neurol* 2011;69(2):400–407.
9. Rolinski M, Griffanti L, Piccini P, et al. Basal ganglia dysfunction in idiopathic REM sleep behaviour disorder parallels that in early Parkinson's disease. *Brain* 2016;139(8):2224–2234.
10. Knudsen K, Fedorova TD, Hansen AK, et al. In-vivo staging of pathology in REM sleep behaviour disorder: a multimodality imaging case-control study [internet]. *Lancet Neurol* 2018;17(7):618–628.
11. Sulzer D, Cassidy C, Horga G, et al. Neuromelanin detection by magnetic resonance imaging (MRI) and its promise as a biomarker for Parkinson's disease [internet]. *NPJ Park Dis* 2018;4(1):11
12. Sasaki M, Shibata E, Tohyama K, et al. Neuromelanin magnetic resonance imaging of locus ceruleus and substantia nigra in Parkinson's disease. *Neuroreport* 2006;17(11):1215–1218.
13. Schwarz ST, Rittman T, Gontu V, et al. T1-weighted MRI shows stage-dependent substantia nigra signal loss in Parkinson's disease. *Mov Disord* 2011;26(9):1633–1638.
14. Castellanos G, Fernández-Seara MA, Lorenzo-Betancor O, et al. Automated Neuromelanin imaging as a diagnostic biomarker for Parkinson's disease [internet]. *Mov. Disord* 2015;30(7):945–952.
15. Cassidy CM, Zucca FA, Girgis RR, et al. Neuromelanin-sensitive MRI as a noninvasive proxy measure of dopamine function in the human brain [internet]. *Proc Natl Acad Sci USA* 2019;116(11):5108–5117.
16. Biondetti E, Gaurav R, Yahia-Cherif L, et al. Spatiotemporal changes in substantia nigra neuromelanin content in Parkinson's disease. *Brain* 2020;143(9):2757–2770.
17. Ronneberger O, Fischer P, Brox T. U-net: convolutional networks for biomedical image segmentation. *Lect Notes Comput Sci* 2015; 9351:234–241. https://doi.org/10.1007/978-3-319-24574-4_28
18. American Academy of Sleep Medicine. The International Classification of Sleep Disorders:(ICSD-3). American Academy of Sleep Medicine; 2014.
19. Hughes AJ, Daniel SE, Kilford L, Lees AJ. Accuracy of clinical diagnosis of idiopathic Parkinson's disease: a clinico-pathological study of 100 cases. *J Neurol Neurosurg Psychiatry* 1992;55(3):181–184.
20. Gaurav R, Yahia-Cherif L, Pyatigorskaya N, et al. Longitudinal changes in Neuromelanin MRI signal in Parkinson's disease. *Mov Disord* 2021;2:9–10.
21. Nichols TE, Holmes AP. Nonparametric permutation tests for functional neuroimaging: a primer with examples. *Hum Brain Mapp* 2002;15(1):1–25.
22. Xing Y, Sapuan A, Dineen RA, Auer DP. Life span pigmentation changes of the substantia nigra detected by neuromelanin-sensitive MRI. *Mov Disord* 2018;33(11):1792–1799.
23. Reimão S, Pita Lobo P, Neutel D, et al. Substantia nigra neuromelanin-MR imaging differentiates essential tremor from Parkinson's disease [internet]. *Mov. Disord* 2015;30(7):953–959.
24. Reimão S, Ferreira S, Nunes RG, et al. Magnetic resonance correlation of iron content with neuromelanin in the substantia nigra of early-stage Parkinson's disease. *Eur J Neurol* 2016;23(2):368–374.
25. Wang J, Huang Z, Li Y, et al. Neuromelanin-sensitive MRI of the substantia nigra: an imaging biomarker to differentiate essential tremor from tremor-dominant Parkinson's disease. *Parkinson's Relat Disord* 2019;58:3–8.
26. Wang J, Li Y, Huang Z, et al. Neuromelanin-sensitive magnetic resonance imaging features of the substantia nigra and locus coeruleus in de novo Parkinson's disease and its phenotypes. *Eur J Neurol* 2018;25(7):949–955.
27. Shinde S, Prasad S, Saboo Y, et al. Predictive markers for Parkinson's disease using deep neural nets on neuromelanin sensitive MRI [internet]. *NeuroImage Clin* 2019;22:101748
28. Le Berre A, Kamagata K, Otsuka Y, et al. Convolutional neural network-based segmentation can help in assessing the substantia nigra in neuromelanin MRI. *Neuroradiology* 2019;61(12):1387–1395.
29. Krupička R, Mareček S, Malá C, et al. Automatic substantia nigra segmentation in neuromelanin-sensitive MRI by deep neural network in patients with prodromal and manifest synucleinopathy. *Physiol Res* 2019;68:S453–S458.
30. Vila M. Neuromelanin, aging, and neuronal vulnerability in Parkinson's disease. *Mov Disord* 2019;34(10):1440–1451.
31. Prasad S, Stezin A, Lenka A, et al. Three-dimensional neuromelanin-sensitive magnetic resonance imaging of the substantia nigra in Parkinson's disease. *Eur J Neurol* 2018;25(4):680–686.
32. Isaias IU, Trujillo P, Summers P, et al. Neuromelanin imaging and dopaminergic loss in parkinson's disease. *Front Aging Neurosci* 2016;8:196
33. Schwarz ST, Xing Y, Tomar P, et al. In vivo assessment of brainstem depigmentation in Parkinson disease: potential as a severity marker for multicenter studies. *Radiology* 2017;283(3):789–798.
34. Kawaguchi H, Shimada H, Kodaka F, et al. Principal component analysis of multimodal neuromelanin MRI and dopamine transporter PET data provides a specific metric for the nigral dopaminergic neuronal density. *PLoS One* 2016;11(3):1–13.
35. Okuzumi A, Hatano T, Kamagata K, et al. Neuromelanin or DaT-SPECT: which is the better marker for discriminating advanced Parkinson's disease? *Eur J Neurol* 2019;26(11):1408–1416.
36. Taniguchi D, Hatano T, Kamagata K, et al. Neuromelanin imaging and midbrain volumetry in progressive supranuclear palsy and Parkinson's disease. *Mov Disord* 2018;33(9):1488–1492.
37. Ohtsuka C, Sasaki M, Konno K, et al. Changes in substantia nigra and locus coeruleus in patients with early-stage Parkinson's disease using neuromelanin-sensitive MR imaging [internet]. *Neurosci. Lett* 2013;541:93–98.
38. Pyatigorskaya N, Magnin B, Mongin M, et al. Comparative study of MRI biomarkers in the substantia nigra to discriminate idiopathic Parkinson disease. *Am J Neuroradiol* 2018;39(8):1460–1467.
39. Oshima S, Fushimi Y, Okada T, et al. Neuromelanin-sensitive magnetic resonance imaging using DANTE pulse. *Mov Disord* 2021; 36(4):874–882.

Supporting Data

Additional Supporting Information may be found in the online version of this article at the publisher's web-site.

SGML and CITI Use Only
DO NOT PRINT

Author Roles

(1) Research project: A. Conception, B. Organization, C. Execution; (2) Statistical Analysis: A. Design, B. Execution, C. Review and Critique; (3) Manuscript: A. Writing of the first draft, B. Review and Critique
RG: 1A; 1B; 1C; 2A; 2B; 3A
NP, EB, RV, LYC, GM,SLS, JCC, MV, IA: 2C; 3B
SL: 1A; 2C; 3A; 3B

Financial Disclosures

Rahul Gaurav and Stéphane Lehéricy received grant funding from Biogen Inc. USA Emma Biondetti received grant funding from France Parkinson and Biogen Inc. USA Romain Valabrègue, Nadya Pyatigorskaya, Graziella Mangone, Lydia Yahia-Cherif, Smaranda Leu-Semenescu and Marie Vidailhet have nothing to report. Jean-Christophe Corvol has served in advisory boards for Air Liquide, Biogen Inc., Denali, Ever Pharma, Idorsia, Prevail Therapeutic, Theranexus, UCB; has received grants from Sanofi and the Michael J Fox Foundation. Isabelle Arnulf received honoraria from Idorsia Pharma, unrelated to this study.